

# Extension of finite volume evolution Galerkin scheme for low Froude number flows based on asymptotic expansion

K. R. Arun

Institut für Geometrie und Praktische Mathematik, RWTH Aachen

`igpm_rwth_logo.pdf`

Numerical Approximations of Hyperbolic Systems with Source Terms and Applications,  
Roscoff, 2011

September 23, 2011

# Let me begin by saying thank you!

- to the collaborators
  - Prof. Dr. Sebastian Noelle,  
RWTH Aachen,
  - Prof. Dr. Maria Lukáčová-Medvidová,  
Johannes Gutenberg-Universität Mainz,
- to all the organisers of this conference,
- to the people paying for me
  - the Alexander von Humboldt Foundation,
- ...and to you all for coming!

## 1 Introduction

- Shallow water equations
- Bicharacteristic evolution operators
- FVEG scheme

- 1 Introduction
  - Shallow water equations
  - Bicharacteristic evolution operators
  - FVEG scheme
- 2 FVEG Scheme for Low Froude Numbers
  - Advection of a vortex
  - Asymptotic analysis

# Outline

- 1 Introduction
  - Shallow water equations
  - Bicharacteristic evolution operators
  - FVEG scheme
- 2 FVEG Scheme for Low Froude Numbers
  - Advection of a vortex
  - Asymptotic analysis
- 3 A Flux-splitting Method
  - A two-grid algorithm

# Outline

- 1 Introduction
  - Shallow water equations
  - Bicharacteristic evolution operators
  - FVEG scheme
- 2 FVEG Scheme for Low Froude Numbers
  - Advection of a vortex
  - Asymptotic analysis
- 3 A Flux-splitting Method
  - A two-grid algorithm
- 4 Numerical Case Studies

# Outline

- 1 Introduction
  - Shallow water equations
  - Bicharacteristic evolution operators
  - FVEG scheme
- 2 FVEG Scheme for Low Froude Numbers
  - Advection of a vortex
  - Asymptotic analysis
- 3 A Flux-splitting Method
  - A two-grid algorithm
- 4 Numerical Case Studies
- 5 Conclusions

# The shallow water system

- System of balance laws

$$\mathbf{u}_t + \mathbf{f}_1(\mathbf{u})_x + \mathbf{f}_2(\mathbf{u})_y = \mathbf{s}(\mathbf{u}, x, y).$$

- Conserved variables and fluxes

$$\mathbf{u} = \begin{pmatrix} h \\ hu \\ hv \end{pmatrix}, \quad \mathbf{f}_1(\mathbf{u}) = \begin{pmatrix} hu \\ hu^2 + \frac{1}{2}gh^2 \\ huv \end{pmatrix}, \quad \mathbf{f}_2(\mathbf{u}) = \begin{pmatrix} hv \\ huv \\ hv^2 + \frac{1}{2}gh^2 \end{pmatrix}.$$

- Source terms

$$\mathbf{s}(\mathbf{u}, x, y) = -gh \begin{pmatrix} 0 \\ b_x \\ b_y \end{pmatrix}.$$



# Linearised system

- Linearised system in primitive variables

$$\mathbf{v}_t + A_1(\tilde{\mathbf{v}})\mathbf{v}_x + A_2(\tilde{\mathbf{v}})\mathbf{v}_y = \mathbf{t}(\tilde{\mathbf{v}}).$$

- Matrix pencil  $A := \cos \theta A_1 + \sin \theta A_2$ .
- Eigenvalues and eigenvectors

$$\lambda_{1,3} = \cos \theta \tilde{u} + \sin \theta \tilde{v} \mp \sqrt{g \tilde{h}}, \quad \lambda_2 = \cos \theta \tilde{u} + \sin \theta \tilde{v}$$

$$\mathbf{l}_{1,3} = \frac{1}{2} \left( \mp 1, \frac{\tilde{c}}{g} \cos \theta, \frac{\tilde{c}}{g} \sin \theta \right), \quad \mathbf{l}_2 = (0, \sin \theta, -\cos \theta)$$

$$\mathbf{r}_{1,3} = \begin{pmatrix} \mp 1 \\ \frac{g}{\tilde{c}} \cos \theta \\ \frac{g}{\tilde{c}} \sin \theta \end{pmatrix}, \quad \mathbf{r}_2 = \begin{pmatrix} 0 \\ \sin \theta \\ -\cos \theta \end{pmatrix}$$

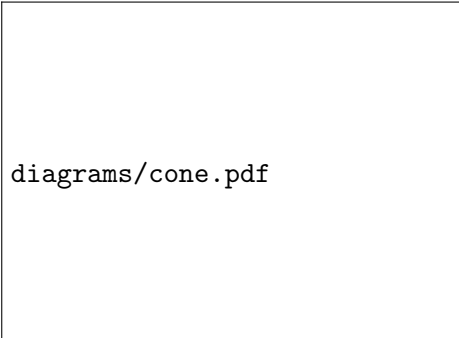
# Bicharacteristics

- Bicharacteristic curves of the linearised system (Courant, Hilbert)

$$\frac{dx}{dt} = \tilde{u} \mp \tilde{c} \cos \theta, \quad \frac{dy}{dt} = \tilde{v} \mp \tilde{c} \sin \theta, \quad \frac{d\theta}{dt} = 0$$

$$\frac{dx}{dt} = \tilde{u}, \quad \frac{dy}{dt} = \tilde{v}, \quad \frac{d\theta}{dt} = 0.$$

- Bicharacteristic cone



diagrams/cone.pdf

# Transport equations

Transport equations along the bicharacteristics

$$-\frac{dh}{dt} + \frac{\tilde{c}}{g} \left( \cos \theta \frac{du}{dt} + \sin \theta \frac{dv}{dt} \right) + \frac{\tilde{c}^2}{g} \left( \sin \theta \frac{\partial u}{\partial \lambda} - \cos \theta \frac{\partial v}{\partial \lambda} \right) = -\tilde{c} \frac{\partial b}{\partial \mu},$$

$$\cos \theta \frac{du}{dt} + \sin \theta \frac{dv}{dt} - g \frac{\partial(h+b)}{\partial \lambda} = 0,$$

$$\frac{dh}{dt} + \frac{\tilde{c}}{g} \left( \cos \theta \frac{du}{dt} + \sin \theta \frac{dv}{dt} \right) - \frac{\tilde{c}^2}{g} \left( \sin \theta \frac{\partial u}{\partial \lambda} - \cos \theta \frac{\partial v}{\partial \lambda} \right) = -\tilde{c} \frac{\partial b}{\partial \mu}.$$

Tangential and normal derivatives  $\partial/\partial\lambda$  and  $\partial/\partial\mu$

$$\frac{\partial}{\partial \lambda} := -\sin \theta \frac{\partial}{\partial x} + \cos \theta \frac{\partial}{\partial y}, \quad \frac{\partial}{\partial \mu} := \cos \theta \frac{\partial}{\partial x} + \sin \theta \frac{\partial}{\partial y}.$$

## Remark

- The derivatives  $d/dt$  are the only ones involving  $\partial/\partial t$ .
- The tangential derivatives can be expressed in terms of  $\partial/\partial\theta$ .

# Exact evolution operators (Lukacova, Noelle, Kraft)

$$\begin{aligned}
 h(P) = & \frac{1}{2\pi} \int_0^{2\pi} \left( h(Q) - \frac{\tilde{c}}{g} u(Q) \cos \theta - \frac{\tilde{c}}{g} v(Q) \sin \theta \right) d\theta \\
 & - \frac{1}{2\pi} \int_{t^n}^{t^{n+1}} \frac{1}{t^{n+1} - \tilde{t}} \int_0^{2\pi} \frac{\tilde{c}}{g} \left( u(\tilde{Q}) \cos \theta + v(\tilde{Q}) \sin \theta \right) d\theta d\tilde{t} \\
 & + \frac{\tilde{c}}{2\pi} \int_{t^n}^{t^{n+1}} \int_0^{2\pi} b_\mu(\tilde{Q}) d\theta d\tilde{t},
 \end{aligned}$$

$$\begin{aligned}
 u(P) = & \frac{1}{2\pi} \int_0^{2\pi} \left( -\frac{g}{\tilde{c}} h(Q) \cos \theta + u(Q) \cos^2 \theta + v(Q) \sin \theta \cos \theta \right) d\theta \\
 & + \frac{1}{2} u(Q_0) - \frac{g}{2} \int_{t^n}^{t^{n+1}} \left( h_x(\tilde{Q}_0) + b_x(\tilde{Q}_0) \right) d\tilde{t} \\
 & + \frac{1}{2\pi} \int_{t^n}^{t^{n+1}} \frac{1}{t^{n+1} - \tilde{t}} \int_0^{2\pi} \frac{\tilde{c}}{g} \left( u(\tilde{Q}) \cos 2\theta + v(\tilde{Q}) \sin 2\theta \right) d\theta d\tilde{t} \\
 & - \frac{g}{2\pi} \int_{t^n}^{t^{n+1}} \int_0^{2\pi} b_\mu(\tilde{Q}) \cos \theta d\theta d\tilde{t}.
 \end{aligned}$$

# Need for a better linearisation

## *Linearisation about a constant state*

- 1 We have linearised the shallow water system about a constant state and the resulting linearised bicharacteristics are always straight lines.
- 2 In many situations, e.g. at low Froude numbers, the gravitational waves travel much faster than the advection waves.
- 3 The fast gravity waves quickly run across the shore and leave the domain, while the nonlinear advection waves slow down and come to halt as they approach the shore.
- 4 In such cases, the nonlinear bicharacteristic cone can have a very anisotropic structure compared to the linearised one.

### *Linearisation about a space dependent state*

- 1 Similar situations arise when the flow behaviour is complex, such as wave run-up over beaches, interaction with solid structures like wave barriers.
- 2 The spatial inhomogeneity in the wave speed causes the diffraction of the bicharacteristics and they no longer remain as straight lines.
- 3 Hence, the idea of linearisation about a constant state may not be satisfactory, and we require a better linearisation, e.g. about a space-dependent state.

# Bicharacteristics

- Linearise the shallow water system about a state  $(u, v, c) = (\tilde{u}, \tilde{v}, \tilde{c})(x, y)$ .

- Evolution of the bicharacteristics are governed by

$$\frac{dx}{dt} = \tilde{u} \mp \tilde{c} \cos \theta, \quad \frac{dy}{dt} = \tilde{v} \mp \tilde{c} \sin \theta, \quad \frac{d\theta}{dt} = -\cos \theta \frac{\partial \tilde{u}}{\partial \lambda} - \sin \theta \frac{\partial \tilde{v}}{\partial \lambda} \pm \frac{\partial \tilde{c}}{\partial \lambda}$$

$$\frac{dx}{dt} = \tilde{u}, \quad \frac{dy}{dt} = \tilde{v}, \quad \frac{d\theta}{dt} = -\cos \theta \frac{\partial \tilde{u}}{\partial \lambda} - \sin \theta \frac{\partial \tilde{v}}{\partial \lambda}$$

## Remark

- *Spatial variation of  $(\tilde{u}, \tilde{v}, \tilde{c})$  is taken into account.*
- *Normal to the wavefront  $(\cos \theta, \sin \theta)$  changes its orientation with time.*
- *In other words, the bicharacteristics diffract.*

# Anisotropic cone

Example of an anisotropic cone (Arun, Kraft, Lukacova, Prasad)

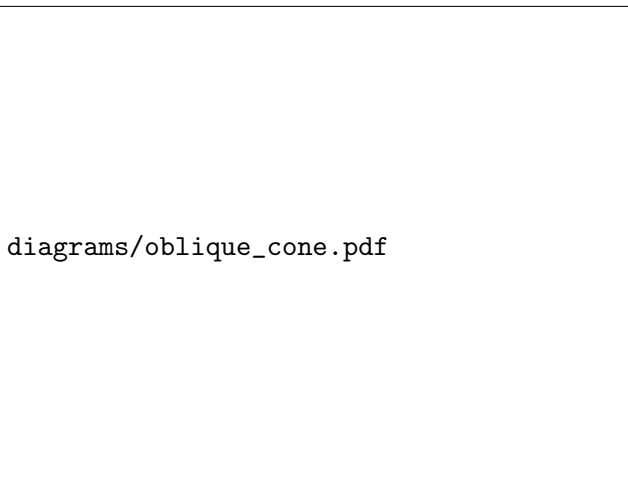


Figure: Anisotropic cone



## Generalised evolution operators

$$\begin{aligned}h(P) &= \frac{1}{2\pi} \int_0^{2\pi} \left( h - \frac{\tilde{c}}{g} u \cos \theta - \frac{\tilde{c}}{g} v \sin \theta \right) (Q) d\omega \\ &\quad - \frac{1}{2\pi g} \int_0^{2\pi} \int_{t^n}^{t^{n+1}} \left\{ \frac{d}{dt} (\tilde{c} \cos \theta) u + \frac{d}{dt} (\tilde{c} \sin \theta) v \right\} (\tilde{Q}) d\tilde{t} d\omega \\ &\quad + \frac{1}{2\pi g} \int_0^{2\pi} \int_{t^n}^{t^{n+1}} \tilde{c}^2 \left( \sin \theta \frac{\partial u}{\partial \lambda} - \cos \theta \frac{\partial v}{\partial \lambda} \right) (\tilde{Q}) d\tilde{t} d\omega \\ &\quad + \frac{1}{2\pi} \int_0^{2\pi} \int_{t^n}^{t^{n+1}} \tilde{c} b_\mu (\tilde{Q}) d\tilde{t} d\omega,\end{aligned}$$

### Remark

*This evolution operator is the generalisation of the ones obtained by Lukacova and collaborators.*

## Generalised evolution operators contd...

$$\begin{aligned}
 u(P) = & \frac{g}{2\pi\tilde{c}(P)} \int_0^{2\pi} \cos \omega \left( -h + \frac{\tilde{c}}{g}u \cos \theta + \frac{\tilde{c}}{g}v \sin \theta \right) (Q) d\omega \\
 & + \frac{1}{2\pi} \int_0^{2\pi} \sin \omega (u \sin \theta - v \cos \theta) (Q_0) d\omega \\
 & + \frac{1}{2\pi\tilde{c}(P)} \int_0^{2\pi} \cos \omega \int_{t^n}^{t^{n+1}} \left\{ \frac{d}{dt}(\tilde{c} \cos \theta)u + \frac{d}{dt}(\tilde{c} \sin \theta)v \right\} (\tilde{Q}) d\tilde{t}d\omega \\
 & + \frac{1}{2\pi} \int_0^{2\pi} \sin \omega \int_{t^n}^{t^{n+1}} \left\{ \frac{d}{dt}(\sin \theta)u - \frac{d}{dt}(\cos \theta)v \right\} (\tilde{Q}_0) d\tilde{t}d\omega \\
 & + \frac{g}{2\pi} \int_0^{2\pi} \sin \omega \int_{t^n}^{t^{n+1}} \frac{\partial(h+b)}{\partial\lambda} (\tilde{Q}) d\tilde{t}d\omega \\
 & - \frac{1}{2\pi\tilde{c}(P)} \int_0^{2\pi} \cos \omega \int_{t^n}^{t^{n+1}} \tilde{c}^2 \left( \sin \theta \frac{\partial u}{\partial \lambda} - \cos \theta \frac{\partial v}{\partial \lambda} \right) (\tilde{Q}) d\tilde{t}d\omega \\
 & - \frac{g}{2\pi\tilde{c}(P)} \int_0^{2\pi} \cos \omega \int_{t^n}^{t^{n+1}} \tilde{c}b_\mu (\tilde{Q}) d\tilde{t}d\omega.
 \end{aligned}$$

## Remarks

- *Exact evolution operators are implicit.*
- *They contain the time integrals of the unknowns and their derivatives.*
- *Integrals along the Mach cone are too complex and to be simplified.*
- *We approximate the time integrals at  $t = t_n$  to get an explicit relation.*
- *Unknown derivatives can be eliminated by integration by parts along the Mach cone.*
- *Leads to the so-called approximate evolution operators.*

Example: approximate evolution operators for the wave equation system

$$\begin{aligned}\phi(P) &= \frac{1}{2\pi} \int_0^{2\pi} (\phi(Q_1) - 2u(Q_1) \cos \theta - 2v(Q_1) \sin \theta) d\theta, \\ u(P) &= \frac{1}{2} u(Q_2) + \frac{1}{2\pi} \int_0^{2\pi} (-\phi(Q_1) \cos \theta + u(Q_1)(3 \cos^2 \theta - 1) \\ &\quad + 3v(Q_1) \sin \theta \cos \theta) d\theta.\end{aligned}$$

# Remarks

- Approximate evolution operators do not depend on the derivatives of  $(h, u, v)$ .
- If one uses a Taylor expansion for prediction, the space derivatives are inevitable.
- Hence, evolution operators are less dependent on the reconstruction of piecewise constant data than the Taylor expansion.
- Integrations along the Mach cone correctly takes into account of the domain of dependence.
- This results in a robust algorithm, particularly for multidimensional problems.

## Theorem (Arun, Noelle)

Suppose that the reconstructions satisfy for all  $x, y$

$$h^n(x, y) + b(x, y) = \text{const}, \quad u^n(x, y) = v^n(x, y) = 0,$$

then the approximate evolution operators satisfy the well-balanced property:

$$\hat{h} + \hat{b} = \text{const}, \quad \hat{u} = \hat{v} = 0.$$

# Finite volume update

- Cartesian grid with cell averages, need to compute fluxes over cell interfaces.
- Choose Gauss quadrature points on the cell interface  $\mathcal{E}$ .
- Construct local Mach cones at the quadrature nodes.
- Use the evolution operator to predict the solution at half time step  $t^{n+\frac{1}{2}} := t^n + \frac{\Delta t}{2}$ .
- Compute the interface flux using

$$\frac{1}{|\mathcal{E}|} \int_{\mathcal{E}} \mathbf{f} \left( \mathbf{u}^{n+\frac{1}{2}} \right) ds = \sum_k \alpha_k \mathbf{f} \left( \mathbf{u}_k^{n+\frac{1}{2}} \right).$$

## Discretisation of source terms

- In each cell, we need to discretise  $-ghb_x$  and  $-ghb_y$ .
- We use same quadrature as used in the flux evaluation.
- In a cell  $C_{i,j}$  we take

$$\mathbf{s}_{i,j}^{n+\frac{1}{2}} = -g \sum_k \alpha_k \begin{pmatrix} 0 \\ \frac{1}{2} \left( \hat{h}_k^r + \hat{h}_k^l \right) \left( \hat{b}_k^r - \hat{b}_k^l \right) \\ \frac{1}{2} \left( \hat{h}_k^t + \hat{h}_k^b \right) \left( \hat{b}_k^t - \hat{b}_k^b \right) \end{pmatrix}$$

# Scheme

Final scheme

$$\mathbf{u}_{i,j}^{n+1} = \mathbf{u}_{i,j}^n - \frac{\Delta t}{\Delta x} \left( \mathcal{F}_{i+\frac{1}{2},j}^{n+\frac{1}{2}} - \mathcal{F}_{i-\frac{1}{2},j}^{n+\frac{1}{2}} \right) - \frac{\Delta t}{\Delta y} \left( \mathcal{F}_{i,j+\frac{1}{2}}^{n+\frac{1}{2}} - \mathcal{F}_{i,j-\frac{1}{2}}^{n+\frac{1}{2}} \right) + \mathbf{s}_{i,j}^{n+\frac{1}{2}}.$$

- Multidimensional generalisation of Godunov's idea to reconstruct, evolve and average.
- Genuine multidimensional flow features are captured very well.
- Very accurate compared to dimension split finite volume schemes.

## Theorem (Lukacova, Noelle, Kraft; Arun, Noelle)

If the predicted values  $(\hat{h}, \hat{u}, \hat{v})$  at the interfaces satisfy

$$\hat{h} + \hat{b} = \text{const}, \quad \hat{u} = \hat{v} = 0,$$

then the above FVEG scheme preserves the steady lake at rest, i.e.

$$h + b \equiv \text{const}, \quad u \equiv v \equiv 0.$$

# Advection of a vortex

- To test the performance of FVEG scheme for low Froude numbers.
- Consider a linearised problem

$$h_t + \tilde{u}h_x + \tilde{v}h_y + \tilde{c}(u_x + v_y) = 0,$$

$$u_t + \tilde{u}u_x + \tilde{v}u_y + \tilde{c}h_x = 0,$$

$$v_t + \tilde{u}v_x + \tilde{v}v_y + \tilde{c}h_y = 0.$$

- Froude number

$$Fr := \frac{\sqrt{\tilde{u}^2 + \tilde{v}^2}}{\tilde{c}}.$$

- Initial velocity: vortex

$$u(x, y, 0) = -\Gamma y e^{\left(\frac{1-r^2}{2}\right)}, \quad v(x, y, 0) = \Gamma x e^{\left(\frac{1-r^2}{2}\right)}.$$

- Vorticity advects with the flow:  $\omega(x, y, t) = \omega(x - \tilde{u}t, y - \tilde{v}t)$ .



# Numerical results

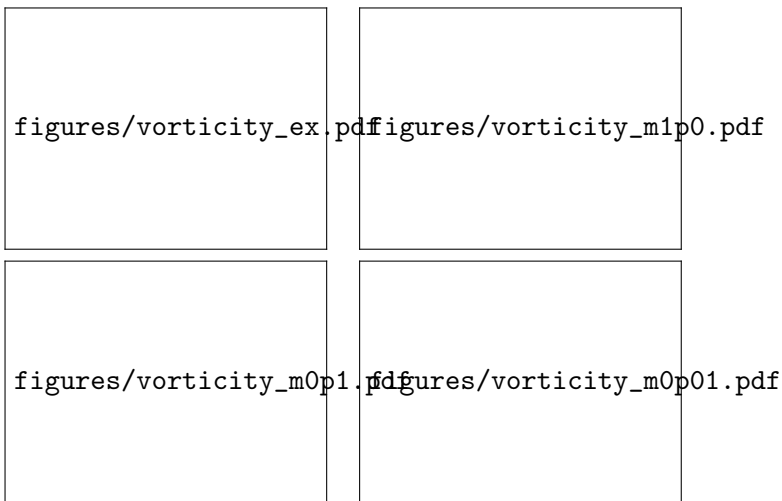



Figure: Advection of a vortex:  $\tilde{u} = 1, \tilde{v} = 0$ . Froude numbers are  $Fr = 1, 0.1, 0.01$ .

## Numerical results contd.



figures/vorticity\_sect.pdf

Figure: Cross section of the vortex along the  $x$ -axis at  $t = 3$ .

## *Numerical simulation of low Mach number flows.*

- Early development: simulation of incompressible flows by Chorin.
- Rigorous convergence results: compressible isentropic flow  $\rightarrow$  incompressible flow by Klainerman and Majda, Schochet, for combustion by Majda and Sethian.
- Difficulties associate with low Froude number:
  - ① Stiffness: disparity in wavespeeds of gravity and advection waves, poses severe restriction on the time-step due to CFL condition.
  - ② Cancellation: water height variable has to accommodate  $\mathcal{O}(1)$  constant height and physically valid  $\mathcal{O}(\varepsilon^2)$  fluctuations, leading to round-off errors.
  - ③ Accuracy: numerical viscosity depends on the Froude number, can cause truncation error to grow as  $\varepsilon \rightarrow 0$ .
- Stiffness issue: Preconditioning approach by Turkel, characteristic time-stepping by vanLeer, Roe and others.

## Developments contd.

- Combination of compressible flow solution and projection methods based on asymptotic expansion by Klein, Munz and coworkers.
- Multiple pressure variable approach:

$$p = p^{(0)} + \varepsilon p^{(1)} + \varepsilon^2 p^{(2)}.$$

- Numerical analysis of Roe-type schemes on Cartesian grids by Guillard and Viozat.
- Analysis of Godunov-type schemes by Dellacherie, Omnes and Rieper.
- Two-grid algorithm due to Le Maître and coworkers.
- Low Mach number scheme of Jin and coworkers.

# Non-dimensional system

Non-dimensional shallow water system: (Le Maître et al.)

$$\begin{aligned}\eta_t + \nabla \cdot ((\eta + h)\mathbf{u}) &= 0, \\ \mathbf{u}_t + \mathbf{u} \cdot \nabla \mathbf{u} + \frac{1}{\varepsilon^2} \nabla \eta &= 0.\end{aligned}$$

- $z = \eta(x, y, t)$ : free surface elevation,
- $z = b(x, y)$ : bottom topography,
- $h = \eta - b$ : water height
- $\mathbf{u}$ : velocity vector.

Reference values:

- $L_{ref}, t_{ref}, u_{ref}$ .
- For gravity waves  $c_{ref} = \sqrt{gh_{ref}}$ .
- Froude number  $\varepsilon := u_{ref}/c_{ref}$ .
- Interested in the regime  $\varepsilon \ll 1$ .

# Asymptotic analysis

- Aim: to identify behaviour of the system as  $\varepsilon \rightarrow 0$ .
- Asymptotic ansatz

$$f(x, t; \varepsilon) = f^{(0)}(x, \xi, t) + \varepsilon f^{(1)}(x, \xi, t) + \varepsilon^2 f^{(2)}(x, \xi, t) + \dots,$$

$$\xi = \varepsilon x.$$

- Multiple space scales and single time scale.
- Use the ansatz for all the unknowns.
- Balancing the powers of  $\varepsilon$  gives the asymptotic equations.

# Summary of asymptotic analysis (Klein, Le Maître et al.)

- Leading order elevation  $\eta^{(0)}$  is constant in space, i.e.  $\eta^{(0)} = \eta^{(0)}(t)$ .
- It can change due to mass flux from boundary:

$$\eta_t^{(0)} = -\frac{1}{|A|} \int_{\partial A} (h + \eta^{(0)}) \mathbf{u}^{(0)} \cdot \mathbf{n} d\sigma.$$

- Leads to a divergence constraint on the leading order momentum

$$\nabla_x \cdot (h + \eta^{(0)}) = -\eta_t^{(0)}.$$

- First order term  $\eta^{(1)}$  does not admit small-scale variations, i.e.  $\eta^{(1)} = \eta^{(1)}(\xi, t)$ .
- It can be interpreted as the amplitude of a gravity wave.
- Large scale components are filtered out by the averaging operator

$$\bar{f}(\xi, t) := \frac{1}{|B(0, \frac{1}{\varepsilon})|} \int_{B(0, \frac{1}{\varepsilon})} f(x, \xi, t) dx.$$

# Summary contd.

- Long scale equations.

$$\eta^{(1)} + \nabla_{\xi} \cdot \overline{(h + \eta^{(0)}) \mathbf{u}^{(0)}} = 0,$$
$$\left( \overline{(h + \eta^{(0)}) \mathbf{u}^{(0)}} \right)_t + \overline{(h + \eta^{(0)}) \nabla_x \eta^{(2)}} = -\overline{(h + \eta^{(0)}) \nabla_{\xi} \eta^{(1)}}.$$

## Remark

- Gravity wavespeed becomes infinite as  $\varepsilon \rightarrow 0$ .
- Large scale derivatives vanish and  $\eta^{(1)}$  becomes constant in space and time.
- Final zero Froude number limit equations cannot contain gravity waves.
- In accordance with Klainerman and Majda.

## Zero Froude number equations

$$\nabla \cdot (\eta + h) \mathbf{u} = -\frac{d\eta}{dt},$$
$$\mathbf{u}_t + \mathbf{u} \cdot \nabla \mathbf{u} + \nabla \eta^{(2)} = 0.$$



# Decomposition

- Conservation form

$$\begin{aligned} H_t + \nabla \cdot H\mathbf{u} &= 0, \\ (H\mathbf{u})_t + \nabla \cdot \left( H\mathbf{u} \otimes \mathbf{u} + \frac{H^2}{2\varepsilon^2} \right) &= \frac{H\nabla h}{\varepsilon^2}, \end{aligned}$$

$$H := (h + \eta).$$

- Splitting into two subsystems:
- 'Fast' subsystem (linear part)

$$\begin{aligned} H_t + \nabla \cdot H\mathbf{u} &= 0, \\ (H\mathbf{u})_t + \nabla \cdot \left( \frac{\eta h}{\varepsilon^2} \right) &= \frac{\eta \nabla h}{\varepsilon^2}. \end{aligned}$$

- 'Slow' subsystem (nonlinear part)

$$\begin{aligned} H_t &= 0, \\ (H\mathbf{u})_t + \nabla \cdot \left( H\mathbf{u} \otimes \mathbf{u} + \frac{\eta^2}{2\varepsilon^2} \right) &= 0. \end{aligned}$$

# Eigenvalues

- Full system

$$\lambda_{1,3} = u \cos \theta + v \sin \theta \mp \frac{\sqrt{h}}{\varepsilon},$$

$$\lambda_2 = u \cos \theta + v \sin \theta.$$

- Fast subsystem

$$\lambda_1 = -\frac{\sqrt{h}}{\varepsilon}, \quad \lambda_2 = 0, \quad \lambda_3 = \frac{\sqrt{h}}{\varepsilon}.$$

- Slow subsystem

$$\lambda_1 = 2u \cos \theta + v \sin \theta, \quad \lambda_2 = 0, \quad \lambda_3 = u \cos \theta + 2v \sin \theta.$$

- Eigenvalues are  $\mathcal{O}\left(\frac{1}{\varepsilon}\right)$  for fast subsystem.
- They are  $\mathcal{O}(1)$  for slow subsystem.
- Both the subsystems are hyperbolic.

# Flux splitting method

- Full system in the quasi one-dimensional case

$$W_t + F_1(W)_x = 0.$$

- Split fluxes

$$F_1(W) = \tilde{F}_1(W) + \hat{F}_1(W),$$

- $\tilde{F}_1$ : fast subsystem,  $\hat{F}_1$ : slow subsystem.
- Finite volume discretisation

$$W_j^{n+1} = W_j^n - \frac{\Delta t}{\Delta x} \left( \mathcal{F}_{j+\frac{1}{2}} - \mathcal{F}_{j-\frac{1}{2}} \right).$$

*Strategy:*

$$\mathcal{F}_{j+\frac{1}{2}} = \tilde{\mathcal{F}}_{j+\frac{1}{2}} + \hat{\mathcal{F}}_{j+\frac{1}{2}}$$

## Contd.

- Since slow system has  $\mathcal{O}(1)$  eigenvalues, we compute the numerical fluxes on a fine grid with mesh size  $\Delta x = \mathcal{O}(1)$ .
- Since the eigenvalues of the fast system are  $\mathcal{O}\left(\frac{1}{\epsilon}\right)$ , numerical fluxes for the fast system are computed on a coarse grid with mesh size  $\Delta \xi = \mathcal{O}\left(\frac{1}{\epsilon}\right)$ .
- Interpolate the coarse fluxes onto the fine grid.

- Time-step for slow system

$$\Delta t_f \frac{\hat{\lambda}_{max}}{\Delta x} = CFL.$$

- Time-step for fast system

$$\Delta t_c \frac{\tilde{\lambda}_{max}}{\Delta \xi} = CFL.$$

- Both  $\Delta t_f$  and  $\Delta t_c$  are  $\mathcal{O}(1)$ .
- Choose

$$\Delta t = \min(\Delta t_f, \Delta t_c).$$

# A test problem (Le Maître et al.)

- One dimensional channel of length  $L_{ref} = 3600Km$  with flat bottom.
- Reference depth  $h_{ref} = 1Km$ .
- Periodic boundary conditions.
- Initial values

$$u(x, 0) = v(x, 0) = 0, \quad \eta(x, 0) = ae^{-\left(\frac{\left(\frac{x}{L_{ref}} - \frac{1}{2}\right)^2}{0.005}\right)},$$

$$a = 0.5m$$

- Linearised solution consists of two waves going to the left and right with speed  $c = \sqrt{gh} \sim 100m/s$ .
- Linearised solution

$$\eta(x, t) = \frac{1}{2} \{ \eta(x - ct) + \eta(x + ct) \}$$

$$u(x, t) = \frac{g}{2c} \{ \eta(x - ct) - \eta(x + ct) \}$$

- Reference velocity  $u_{ref} = ga/c = 0.05m/s$ .
- Froude number  $\varepsilon = u_{ref}/c_{ref} = 5 \times 10^{-4}$ .

## setup contd.

- Use 360 fine mesh points, i.e.  $\Delta x = 10Km$ .
- Coarse mesh size  $\Delta \xi = r \Delta x = 30Km$ , i.e.  $r = 3$ .
- First order Lax-Friedrichs numerical fluxes.
- Euler time-stepping.
- $CFL = 0.95$
- Linear interpolation of coarse flux-differences onto the fine grid.
- After each time step, solution is smoothed using

$$W_j \rightarrow \frac{1}{2} (W_{j-1} + W_{j+1})$$

### Remark

*Without smoothing, the solution contains high frequency oscillations!*

figures/elevation\_t0t4.pdf

**Figure:** Surface elevation computed using the split scheme. Final time  $t = 4Hrs$

# Results

- Effect of grid coarsening.

figures/elevation\_r3.pdf

figures/elevation\_r6.pdf

Figure: Effect of grid coarsening



figures/elevation\_r12.pdf

figures/elevation\_r24.pdf

Figure: Effect of grid coarsening

## *FVEG scheme for shallow water equations*

- Generalised evolution operators are derived by considering a space dependent linearisation state.
- Evolution operators are approximated using appropriate numerical quadratures.
- Approximate evolution operators satisfy the conditions for well-balancing.
- Well-balanced genuinely multidimensional FVEG scheme is derived using the approximate evolution operators.

### *Flux-splitting scheme for low Froude number*

- Conservative hyperbolic splitting is introduced.
- Guided by the asymptotic considerations, the shallow water system is split into two subsystems.
- Wave velocities of the 'fast' subsystem are  $\mathcal{O}(\frac{1}{\epsilon})$  and that of 'slow' system are  $\mathcal{O}(1)$ .
- Two-grid algorithm based on fine-coarse grid is proposed.
- Numerical fluxes are evaluated on different grids.
- Fluxes are assembled to get the flux on a single grid.
- Two-grid algorithm overcomes the stiffness due to CFL restriction.

## Future work

- Two-grid framework has to be incorporated to the FVEG scheme.
- The method has to be validated against benchmark problems in multidimensions.
- Include nonzero bottom topography and study its influence on the propagation of long waves.
- Well-balancing has to be introduced in the new framework.
- Efficient filtering has to be introduced to remove the high frequency oscillations.
- Better flux interpolation strategies.
- Extension to high order accuracy.

*Thank You for Your Kind Attention!*